Evaluation of ruthenium-based complexes for the controlled radical polymerization of vinyl monomers

François Simal, Dominique Jan, Lionel Delaude, Albert Demonceau, Marie-Rose Spirlet, and Alfred F. Noels

Abstract: New complexes of the type $RuCl_2$(*p*-cymene)L where the ligand L is either a phosphine or a stable triazolinylidene carbene have been tested and compared to the Grubbs' benzylidene complex $RuCl_2(=CHPh)(PCy_3)_2$ as catalyst precursors for the controlled atom transfer radical polymerization (ATRP) of methyl methacrylate and of various *para*-substituted styrenes. Kinetic data and Hammett ρ constants are reported, as well as the X-ray structure of the *ortho*-metallated triazolinylidene-ruthenium(II) complex RuCl(*p*-cymene)[1,2-phenylene[3,4-diphenyl-1*H*-1,2,4-triazol-1-yl-5(4*H*)-ylidene]].

Key words: ruthenium, carbene, chelate complex, homogeneous catalysis, atom transfer radical polymerization.

Résumé : De nouveaux complexes du type $RuCl_2$(*p*-cymène)L où le ligand L désigne une phosphine ou un carbène triazolinylidène ont été testés et comparés au complexe benzylidène de Grubbs $RuCl_2(=CHPh)(PCy_3)_2$ comme précurseurs de catalyseurs pour la polymérisation radicalaire contrôlée par transfert d'atome (ATRP) du méthacrylate de méthyle et de divers styrènes *para*-substitués. Des données cinétiques et les constantes de Hammett ρ sont rapportées ainsi que la structure cristallographique du complexe ruthénium(II)-triazolinylidène *ortho*-métallé RuCl(*p*-cymène)[1,2-phénylène[3,4-diphényl-1*H*-1,2,4-triazol-1-yl-5(4*H*)-ylidène]].

Mots clés: ruthénium, carbène, complexe chélaté, catalyse homogène, polymérisation radicalaire par transfert d'atome.

Introduction

The advent of well-defined organometallic complexes which may be used as initiators for controlled radical polymerization has opened new vistas in macromolecular synthesis. A major advance in this field came from the development of the so-called atom transfer radical polymerization (ATRP), which takes advantage of the redox properties of transition-metals (1–3). ATRP is based on a dynamic equilibration between active propagating radicals and dormant species. This equilibrium is established through the reversible transition-metal-catalyzed homolytic cleavage of the covalent carbon—halogen bond in the dormant species (Scheme 1) (4).

Catalytic engineering at the metal center aims to shift this equilibrium toward the dormant species. Thus, the concentration of propagating radicals remains low thorough the whole polymerization process and a high degree of control ensues, allowing not only the synthesis of polymers of predictable molecular weights and low polydispersities, but also the preparation of novel, functionalized, block copolymers amenable to further transformations (5, 6).

Polymerization systems utilizing the ATRP concept have been developed with complexes of Cu, Ru, Ni, Pd, Rh, and Fe during the last five years (7–10). We recently reported on the exceptional efficiency and versatility of new catalysts based on $RuCl_2$(*p*-cymene)(PR_3) (**1**) for promoting the ATRP of vinyl monomers (*p*-cymene is 4-isopropyltoluene) (11). The choice of the phosphane ligand proved to be crucial. Only phosphanes which were both strongly basic and which possessed a well-defined steric bulk led to both high catalytic activity and high control of the polymerization process (high initiation efficiency f and narrow molecular weight distribution, M_w/M_n = 1.1). Along these guidelines, the most suitable phosphines in our hands were tricyclohexylphosphine (PCy_3) and triisopropylphosphine (P-*i*-Pr_3). The corresponding catalyst precursors **1** are conveniently and quantitatively prepared by reacting the ruthenium dimer $[RuCl_2(p\text{-cymene})]_2$ with 2 equiv of the phosphine (12, 13). They exhibit a high tolerance to heteroatom functionality in

Received August 8, 2000. Published on the NRC Research Press Web site at http://canjchem.nrc.ca on May 30, 2001.

Dedicated to Professor Brian James on the occasion of his 65th birthday.

F. Simal, D. Jan, L. Delaude, A. Demonceau, and A.F. Noels.[1] Center for Education and Research on Macromolecules (CERM), Institut de Chimie (B6a), Université de Liège, Sart-Tilman, B-4000 Liège, Belgium.
M.-R. Spirlet. Physique expérimentale, Institut de Physique (B5), Université de Liège, Sart-Tilman, B-4000 Liège, Belgium.

[1] Corresponding author (telephone: +32 (4) 366-3463; fax: +32 (4) 366-3497; e-mail: AF.Noels@ulg.ac.be).

DOI: 10.1139/cjc-79-5/6-529

Scheme 1.

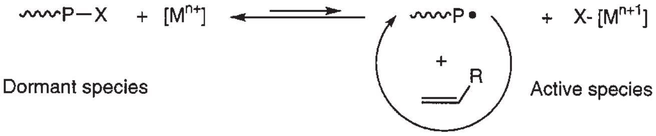

the monomer, as well as to ubiquitous impurities such as oxygen and water.

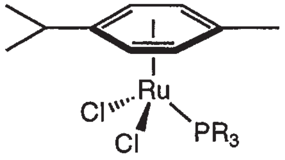

1

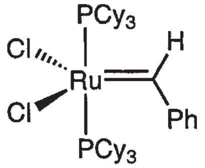

2

Surprisingly, the best catalysts for ATRP were also the most active ones for the ring-opening metathesis polymerization (ROMP) of cycloolefins, a reaction where metal–carbene moieties (in equilibrium with metallacyclobutanes) are known to play a key role (14). This prompted us to test preformed metal–carbene complexes such as $RuCl_2(=CHPh)(PCy_3)_2$ (**2**) — a ruthenium-benzylidene catalyst precursor commonly used for olefin metathesis (15) — under ATRP conditions (16). The results were most gratifying and we further expanded our investigations in this field by substituting *N*-heterocyclic stable carbenes for the phosphine ligands (17).

In this article, we present further studies on the scope and limitations of: (*i*) new arene–ruthenium(II)-phosphine complexes; and (*ii*) new arene–ruthenium(II)-triazolinylidene complexes as potential catalysts for the controlled radical polymerization of methyl methacrylate (MMA) and of substituted styrenes.

Results and discussion

Polymerization of MMA with $RuCl_2$(*p*-cymene)PR_3 catalyst precursors

In a previous communication from our group, the catalytic activity of numerous $RuCl_2$(*p*-cymene)PR_3 complexes based on trialkyl-, triaryl-, or mixed alkylarylphosphines was investigated under ATRP conditions. Methyl methacrylate was chosen as a model substrate and polymerizations were initiated by ethyl 2-bromo-2-methylpropanoate at 85°C (11). Ruthenium–arene complexes containing the tricyclohexylphosphine (**1a**) and, to a slightly lesser extent, triisopropylphosphine (**1b**) emerged from this study as the most efficient catalyst precursors.

To complement our initial screening, we have tested new complexes based on tricyclopentylphosphine (**1c**), *tert*-butyldicyclohexylphosphine (**1d**), and dicyclohexylphosphine (**1e**) using the same experimental conditions for MMA polymerization. The results are summarized in Table 1. For comparison sake, data previously obtained with **1a** ($PR_3 = PCy_3$) and **1b** (PR_3 = P-*i*-Pr_3) are also included.

Table 1. Polymerization of methyl methacrylate with various $RuCl_2$(*p*-cymene)PR_3 catalyst precursors.[a]

Catalyst	PR_3	Polymer yield (%)	M_n (kg mol^{-1})[b]	M_w/M_n	f [c]
1a	PCy_3	100	41.5	1.12	0.95
1b	P-*i*-Pr_3	80	40.5	1.10	0.8
1c	PCp_3	99	66	1.12	0.6
1d	PCy_2-*t*-Bu	99	63	1.14	0.65
1d[d]	PCy_2-*t*-Bu	84	45	1.11	0.75
1e	PCy_2H	32	150	1.8	0.1

[a] Reaction conditions: MMA 1 mL, initiator (ethyl 2-bromo-2-methylpropanoate) 0.0234 mmol, catalyst 0.0117 mmol, 16 h at 85°C.

[b] Determined by size-exclusion chromatography with PMMA calibration.

[c] Initiation efficiency $f = M_{n,\text{ theor.}}/M_{n,\text{ exp.}}$ with $M_{n,\text{ theor.}} = ([\text{monomer}]_0/[\text{initiator}]_0) \times \text{MW (monomer)} \times \text{conversion}$.

[d] Reaction at 60°C.

Both PCp_3 and PCy_2-*t*-Bu fulfill the requirements previously defined for achieving a high catalytic activity, namely a strong basicity and a well-defined steric bulk ($160° < \theta < 170°$, θ = cone angle of the phosphine). Accordingly, complexes **1c** and **1d** are more than satisfactory catalyst precursors for MMA polymerization. On the other hand, PCy_2H is a much less efficient ligand, probably because of its smaller cone angle (θ = 143°) (18) and weaker basicity (pK_a $H_2PCy_2^+ = 4.55$) (19) compared to PCy_3 (θ = 170°, pK_a $HPCy_3^+ = 9.70$).

A detailed examination of the polymerization kinetics reveals that complexes based on the PCy_3 or PCp_3 ligands deserve the title of best catalyst precursors, because they display slightly faster reaction rates and afford better molecular weight control than the ones ligated to P-*i*-Pr_3 or PCy_2-*t*-Bu. For instance, the apparent propagation constants k_p^{app} calculated for **1a** and **1d** are 1.05×10^{-4} s^{-1} and 7.9×10^{-5} s^{-1}, respectively. Data analysis also confirms the living nature of the polymerization process with the most efficient catalytic systems. The plots of ln $([M]_0/[M])$ and of M_n vs. monomer conversion are linear (not shown), and polymerization resumes when a second feed of MMA is added to an (almost) completely polymerized reaction mixture. Last but not least, the polymer samples were all colorless after a single precipitation step, a feature that catalytic systems based on other types of transition-metal complexes often lack (10, 20).

Polymerization of styrene and of *p*-substituted styrenes with $RuCl_2$(*p*-cymene)PR_3 catalyst precursors

To broaden the scope of our study on ruthenium(II)-phosphine complexes, a comparison of various catalyst precursors for the polymerization of different *para*-substituted styrenes was carried out. Prior reports strongly suggest that the same stereoelectronic requirements for the phosphine ligand apply to the polymerization of styrene and of MMA (11,21). Therefore, we have tested only three $RuCl_2$(*p*-cymene)PR_3 complexes which contain sterically demanding basic phosphines, viz. **1a** ($PR_3 = PCy_3$), **1b** (PR_3 = P-*i*-Pr_3), and **1d** ($PR_3 = PCy_2$-*t*-Bu). The polymerization of unsubstituted styrene initiated by ethyl 2-bromopropanoate at 110°C served as a model reaction in a first set of experiments. A comparative run in the presence of the Grubbs' benzylidene catalyst **2** was included and the results are summarized in Table 2.

Table 2. Polymerization of styrene with various $RuCl_2$(*p*-cymene)PR_3 and $RuCl_2(=CHPh)(PCy_3)_2$ catalyst precursors.[a]

Catalyst	PR_3	Polymer yield (%)	M_n (kg mol^{-1})[b]	M_w/M_n	f[c]
1a	PCy_3	58	27	1.25	0.85
1b	P-*i*-Pr_3	45	18	1.11	0.95
1d	PCy_2-*t*-Bu	57	23.5	1.85	0.95
2	PCy_3	61	27	1.38	0.9

[a] Reaction conditions: styrene 1 mL, initiator (ethyl 2-bromopropanoate) 0.0234 mmol, catalyst 0.0117 mmol, 16 h at 110°C.

[b] Determined by size-exclusion chromatography with PS calibration.

[c] See footnote *c*, Table 1 for a definition of *f*.

Table 3. Polymerization of styrene and of *p*-substituted styrenes with $RuCl_2$(*p*-cymene)PCy_3 as catalyst precursor.[a]

Monomer	Polymer yield (%)	M_n (kg mol^{-1})[b]	M_w/M_n	k_p^{app} (1×10^5 s^{-1})
4-Chlorostyrene[c]	68	18	1.27	2.01
Styrene	58	27	1.25	1.52
4-Methylstyrene	45	16	1.38	0.97
4-Methoxystyrene[c]	51	1.4	2.5	1.11

[a] Reaction conditions: 4-X-styrene 1 mL, initiator (ethyl 2-bromopropanoate) 0.0234 mmol, catalyst (**1a**) 0.0117 mmol, 16 h at 110°C.

[b] Determined by size-exclusion chromatography with PS calibration.

[c] Reaction time 24 h.

Fig. 1. Hammett plot for the polymerization of *p*-substituted styrenes initiated by ethyl 2-bromopropanoate and mediated by $RuCl_2$(*p*-cymene)PCy_3 at 110°C.

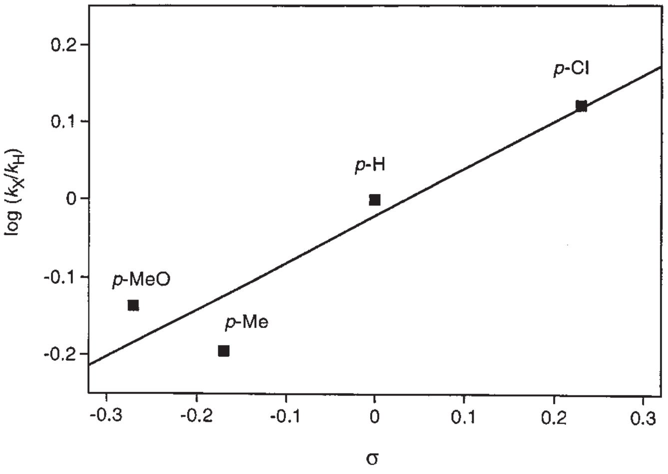

Although styrene is less prone to ATRP than MMA, catalysts **1a**, **b**, **d**, and **2** permit a moderate to satisfactory control of its polymerization. The narrowest molecular weight distribution was obtained with complex **1b**, while Grubbs' benzylidene complex **2** displayed the fastest reaction kinetics. Thus, the apparent propagation constants k_p^{app} (expressed in 10^5 s^{-1}) follow the order: 1.85 (**2**) > 1.52 (**1a**) > 1.25 (**1d**) > 1.16 (**1b**). In all cases, a linear relationship was observed between the number-average molecular weight (M_n) of the polystyrene samples and the monomer conversion.

To gain further insight into the reaction mechanism and kinetics, the polymerization of various *para*-substituted styrenes was carried out at 110°C with ethyl 2-bromopropanoate as initiator. The results obtained with styrene, 4-chloro-, 4-methyl-, and 4-methoxystyrene are listed in Table 3. They clearly show that the polymerization process is favored when an electron-withdrawing group is present on the aromatic ring. The relative reaction rates k_X/k_H follow the sequence: 1.32 (4-chlorostyrene) > 1 (styrene) > 0.73 (4-methoxystyrene) > 0.63 (4-methylstyrene). The decrease in rates is furthermore associated with an increase in the polydispersity ratio M_w/M_n.

No high molecular weight polymer was formed with 4-methoxystyrene, although the monomer conversion reached ca. 50%. This indicates that transfer reactions take over propagation, a likely consequence of competing ionic processes induced by the electron-donating substituent on styrene that could favor the heterolytic cleavage of the carbon—halogen bond in the active species. Yet, we opted for not excluding the data acquired with *p*-methoxystyrene from the Hammett plot presented in Fig. 1. With all four points, the correlation between log (k_X/k_H) and the substituent σ constant (22) leads to a ρ value of 0.60 and a correlation coefficient of 0.93. The ρ value becomes 0.78 when the 4-methoxy point is discarded, but the conclusion remains the same: one is dealing with a *nucleophilic* active radical species which favors the polymerization of electron-poor olefins.

Synthesis and evaluation of new RuCl(*p*-cymene)(triazolinylidene) catalyst precursors

In this section, we describe our attempts at further improving the ATRP of vinyl monomers by replacing the phosphine ligands in ruthenium complexes with *N*-heterocyclic carbenes (NHC). These new, stable, nucleophilic divalent carbon species are increasingly used in organometallic synthesis (23). They are very strong σ-donating ligands, while the extent of their π-back-bonding is negligible. Many representatives of this new class of compounds isolated so far also bear large substituents, such as benzyl or mesityl groups, on the ring nitrogen atoms. Because of these combined electron-donating properties and steric bulkiness, *N*-heterocyclic carbenes seemed to us to be promising alternatives to strongly basic, sterically crowded phosphines as ligands in our catalyst precursors.

Presently, derivatives of the imidazole and of the triazole ring systems constitute the most widely studied NHC. Our investigations concerning the diaza heterocyclic ligands have been reported elsewhere (17) and we shall focus here solely on the use of a commercially available triazolinylidene carbene, viz. 1,3,4-triphenyl-4,5-dihydro-1*H*-1,2,4-triazol-5-ylidene (**3**) (24). The stoichiometric reaction between this ligand and the ruthenium dimer $[RuCl_2(p\text{-cymene})]_2$ is depicted in Scheme 2. The addition of a base (EtN-*i*-Pr_2 in excess) is required to obtain selectively and quantitatively a single adduct. Indeed, the reaction proceeds via the opening of the μ-chloro bridges of the dimer and the coordination of the incoming carbene to the ruthenium atom. An *ortho*-metallation of the phenyl substituent in position 1 occurs and 1 equiv of HCl is released. It is trapped by the base, which therefore helps driving the reaction to its completion and prevents side-reactions between the protic acid and the highly reactive free carbene species.

Scheme 2.

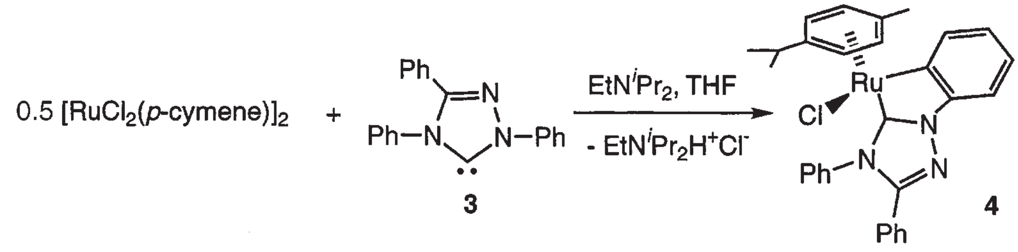

Table 4. Selected bond distances (Å) and bond angles (°) for complex **4**.

Bond distances (Å)					
Ru—Cl	2.4187(8)	Ru—C(4)	2.284(3)	Ru—C(7)	2.198(3)
Ru—C(1)	2.004(3)	Ru—C(5)	2.185(3)	Ru—C(8)	2.267(3)
Ru—C(3)	2.300(3)	Ru—C(6)	2.207(3)	Ru—C(30)	2.071(3)
Bond angles (°)					
Cl-Ru-C(1)	84.06(8)				
Cl-Ru-C(30)	87.63(8)				
C(1)-Ru-C(30)	76.77(11)				

Fig. 2. Molecular structure of complex **4** showing the numbering system; ORTEP diagram with 50% probability ellipsoids.

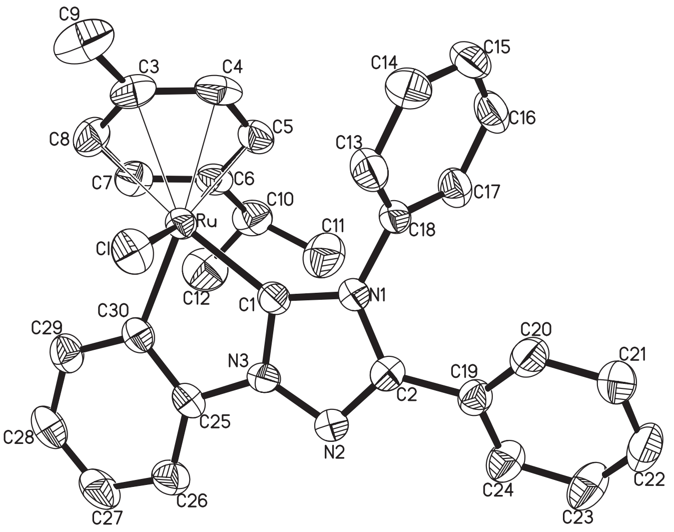

Complex **4** was isolated as a yellow, air- and water-stable powder and its structure in the solid state was determined by X-ray crystallography. A plot of its molecular structure and a listing of selected bond distances and bond angles are reported in Fig. 2 and Table 4, respectively.

The structure of **4** is close to that reported by Enders et al. (25) for similar complexes. The ruthenium atom lies in a *pseudo*-tetrahedral environment, and the C(1)-Ru-C(30) angle formed between the metal and the two carbon atoms from the chelating ligand equals 76.11(11)° (see Fig. 2 for atom numbering). The triazolinylidene ring is planar and the interatomic distances are in agreement with those observed in other ruthenium–nucleophilic carbene complexes (26, 27). The ruthenium-carbene carbon bond length is 2.004(3) Å, and the *ortho*-metallation takes place with the phenyl ring located at N(3) rather than N(1). At 2.071(3) Å the ruthenium-carbon σ bond to the phenyl ring (Ru—C(30)) is comparable to the values obtained for other *ortho*-metallated *N*-arylcarbenes (25). Furthermore, the *p*-cymene ligand is tilted, the distances ruthenium to C(8), C(3), and C(4) (2.267(3)–2.300(3) Å) are longer than the distances ruthenium to C(7), C(6), and C(5) (2.185(3)–2.207(3) Å). We attribute this distortion to a relatively important *trans* effect of the *ortho*-metallated carbene ligand.

^{1}H and ^{13}C NMR spectra corroborate the X-ray analysis and bring over additional structural information on complex **4** (see *Experimental section* for detailed assignments). The carbene-carbon resonates at 192.8 ppm, a typical value for this type of complex. Due to chirality, all aromatic hydrogen and carbon atoms from the *p*-cymene ligand are inequivalent. The aromatic protons appear as 2 AB systems and the aromatic carbons as 6 different singlets in ^{1}H and proton-decoupled ^{13}C NMR spectra, respectively. The two methyls from the isopropyl group give rise to two doublets (^{1}H NMR) or two singlets (^{13}C NMR). No changes in the NMR spectra were observed even at temperatures as high as 110°C, indicating that dissociation of the *p*-cymene ligand does not take place under these conditions.

Addition of 1 equiv of silver tetrafluoroborate to the neutral complex **4** led to the corresponding cationic species **5** ligated to an extra molecule of solvent (CH_3CN) (Scheme 3). As expected, the cationic complex displayed after purification the same NMR characteristics than its neutral precursor, i.e., inequivalent C and H atoms for the arene ligand.

Both **4** and **5** were tested as ATRP catalysts. Cationic complex **5** was practically inactive at promoting the polymerization of MMA and of styrene, whereas its neutral counterpart **4** proved to be an active catalyst precursor for the ATRP of vinyl monomers. Because a reversible oxidation of Ru(II) into Ru(III) is central to the ATRP mechanism (cf. Scheme 1), one could argue that the already charged species **5** is less prone to oxidation than its neutral counterpart **4**, thus explaining the large difference in reactivity between the two of them. Results obtained with MMA, styrene, and two *para*-substituted styrenes using complex **4**

Scheme 3.

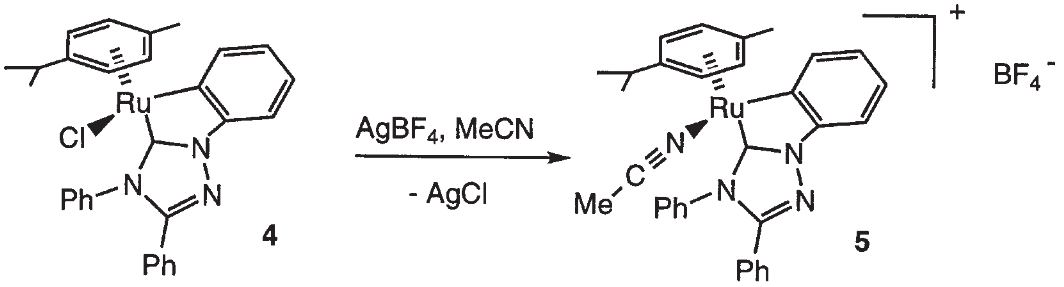

Table 5. Polymerization of methyl methacrylate and of styrenes mediated by complex **4**.

Monomer	Polymer yield (%)	M_n (kg mol^{-1})[a]	M_w/M_n	f[b]
MMA[c]	80	56.5	1.6	0.55
Styrene[d]	81	35	1.4	0.9
4-Chlorostyrene[d]	83	42	1.5	0.98
4-Methylstyrene[d]	80	38.5	1.5	0.8

[a] Determined by size-exclusion chromatography with PMMA or PS calibration.
[b] See footnote *c*, Table 1 for a definition of *f*.
[c] Reaction conditions: MMA 1 mL, initiator (ethyl 2-bromo-2-methylpropanoate) 0.0234 mmol, catalyst (**4**) 0.0117 mmol, 16 h at 85°C.
[d] Reaction conditions: 4-X-styrene 1 mL, initiator ((1-chloroethyl)benzene) 0.0234 mmol, catalyst (**4**) 0.0117 mmol, 16 h at 110°C.

as catalyst precursor are summarized in Table 5. Standard polymerization conditions were applied with ethyl 2-bromo-2-methylpropanoate and (1-chloroethyl)benzene as initiators for MMA and styrenes, respectively.

The molecular weight distributions are slightly narrower for polystyrenes than for PMMA. However, the *ortho*-metallated triazolinylidene complex **4** does not afford a better control of the polymerization than the phosphine-based catalysts **1a**–**d**. It also loses more rapidly its efficiency when the reaction temperature is lowered, since the polymer yield drops to 16% when MMA is reacted at 75°C instead of 85°C and no more PMMA is isolated when the reaction is carried out at 60°C. Thus, catalyst **4** is presently no match for complexes **1** and **2**, whose synthesis is also more straightforward. Further studies concerning the relationship between ATRP and ATRA (atom transfer radical addition, Kharasch reaction) as a function of the electronic tuning and other variations of the carbene ligand are in progress.

Experimental Section

General information

All the solvents and monomers were dried, distilled, and degassed prior to use. They were stored under nitrogen at –20°C in the absence of light. NMR spectra were recorded on a Brucker AM 400 spectrometer (400 and 100 MHz for ^{1}H and ^{13}C NMR, respectively). Chemical shifts are listed in ppm downfield from TMS with the solvent as the internal standard. Infrared spectra were recorded on a PerkinElmer 1720X series FT-IR spectrometer from KBr discs. Elemental analyses were performed at the Laboratory of Pharmaceutical Chemistry, University of Liège.

Materials

Complexes **1a**–**e** were prepared according to the literature (12, 13). $RuCl_2(=CHPh)(PCy_3)_2$ (**2**) was used as received from Strem. 1,3,4-Triphenyl-4,5-dihydro-1*H*-1,2,4-triazol-5-ylidene (**3**) was purchased from Acros.

*Chloro[(1,2,3,4,5,6-η)-1-methyl-4-(1-methylethyl) benzene][1,2-phenylene[3,4-diphenyl-1*H*-1,2,4-triazol-1-yl-5(4*H*)-ylidene]]ruthenium (**4**)*

A 0.44 g sample of 1,3,4-triphenyl-4,5-dihydro-1*H*-1,2,4-triazol-5-ylidene **3** (0.48 mmol) was weighted in a glove box and dissolved in 15 mL of THF. This solution was added via a cannula to a mixture of $[RuCl_2(p\text{-cymene})]_2$ (0.40 g, 0.65 mmol) and *N*,*N*-diisopropylethylamine (0.75 g, 5.74 mmol) in 40 mL of THF under inert atmosphere. The initial red suspension was stirred 4.5 h at room temperature. It progressively turned into an orange then a yellow solution. After 4.5 h the solvent was removed on a rotary evaporator and the yellow residue was purified by column chromatography on silica gel with CH_2Cl_2. The eluate was washed with H_2O (3 × 20 mL) to remove the ammonium salt, dried over sodium sulfate, and evaporated. The residue was rinsed with Et_2O (2 × 10 mL) and *n*-pentane (2 × 15 mL) to afford the title compound as a bright yellow powder. Yield: 0.59g (79%); mp 215°C (dec.). IR (cm^{-1}): 3052(m), 2959(m), 2915(m), 2865(m), 1593(m), 1533(m), 1497(s), 1143(s), 1336(s), 1013(m), 750(s), 702(s). ^{1}H NMR ($CDCl_3$, δ ppm): 8.13 (d, 1H, C*H* Ph, $^3J_{H\text{-}H}$ = 8.4 Hz), 7.60–7.31 (m, 11H, C*H* Ph), 7.05 (t, 2H, C*H* Ph, $^3J_{H\text{-}H}$ = 5.0 Hz), 5.43 (d, 1H, C*H* *p*-cym, C*H* Ph, $^3J_{H\text{-}H}$ = 6.4 Hz), 5.19 (d, 1H, C*H* *p*-cym, C*H* Ph, $^3J_{H\text{-}H}$ = 6.4 Hz), 4.63 (d, 1H, C*H* *p*-cym, C*H* Ph, $^3J_{H\text{-}H}$ = 6.4 Hz), 4.55 (d, 1H, C*H* *p*-cym, C*H* Ph, $^3J_{H\text{-}H}$ = 6.4 Hz), 2.12 (sept, 1H, C*H*CH_3, $^3J_{H\text{-}H}$ = 6.8 Hz), 1.92 (s, 3H, ArCH_3), 0.83 (d, 3H, CHCH_3, $^3J_{H\text{-}H}$ = 6.8 Hz), 0.66 (d, 3H, CHCH_3, $^3J_{H\text{-}H}$ = 6.8 Hz). ^{13}C NMR ($CDCl_3$, δ ppm): 192.81 (Ru=*C*), 160.78 (Ru-C_{ar}), 152.06 (N-C_{ar}), 144.76 (N-C_{ar}), 141.30 (=C-C_{ar}), 137.47, 131.03, 130.27, 128.88, 127.36, 125.51, 125.37, 122.59, 121.96, 112.93 (Ph), 105.07, 99.81 ($C_{ar}CH_3$, $C_{ar}CH(CH_3)_2$), 93.12, 90.57, 89.80, 82.60 (*C*H *p*-cym), 30.88 (*C*HMe$_2$), 23.34 ($CH(CH_3)_2$), 21.16 ($CH(CH_3)_2$), 18.89 (Ar*C*H_3 *p*-cym). Anal. calcd. for $C_{30}H_{28}ClN_3Ru$ (%): C 63.53, H 4.95, N 7.41; found: C 63.13, H 5.40, N 7.48.

*(Acetonitrile)[(1,2,3,4,5,6-η)-1-methyl-4-(1-methylethyl)benzene][1,2-phenylene[3,4-diphenyl-1H-1,2,4-triazol-1-yl-5(4*H*)-ylidene]]ruthenium tetrafluoroborate (**5**)*

Complex **4** (151 mg, 0.266 mmol) and $AgBF_4$ (104 mg, 0.532 mmol) were dissolved in 40 mL of acetonitrile under nitrogen. The initial yellow suspension was stirred 18 h at room temperature. It progressively turned into a green then a purple solution. After 18 h the mixture was filtered on a Celite pad and the solvent was removed on a rotary evaporator. The blue residue was purified by column chromatography on silica gel (eluent CH_2Cl_2:CH_3OH, 10:1). Evaporation of the eluent afforded **5** as a blue powder which was rinsed with Et_2O (3 × 20 mL) and dried. Yield: 0.13 g (76%); mp 140°C (dec.). IR (cm^{-1}): 3055(w), 2964(w), 2930(w), 1596(w), 1498(m), 1446(m), 1399(m), 1338(m), 1262(m), 1062(s), 700(m). ^{1}H NMR (CD_2Cl_2, δ ppm): 8.00 (d, 1H, C*H* Ph, $^3J_{\text{H-H}}$ = 6.4 Hz), 7.73–7.09 (m, 13H, C*H* Ph), 5.60 (d, 1H, C*H* *p*-cym, C*H* Ph, $^3J_{\text{H-H}}$ = 6.2 Hz), 5.37 (d, 1H, C*H* *p*-cym, C*H* Ph, $^3J_{\text{H-H}}$ = 6.2 Hz), 5.04 (d, 1H, C*H* *p*-cym, C*H* Ph, $^3J_{\text{H-H}}$ = 6.2 Hz), 4.94 (d, 1H, C*H* *p*-cym, C*H* Ph, $^3J_{\text{H-H}}$ = 6.2 Hz), 2.22 (s, 3H, CH_3CN), 2.12 (sept, 1H, C*H*CH_3, $^3J_{\text{H-H}}$ = 6.4 Hz), 1.93 (s, 3H, ArCH_3), 0.84 (d, 3H, CHCH_3, $^3J_{\text{H-H}}$ = 6.4 Hz), 0.73 (d, 3H, CHCH_3, $^3J_{\text{H-H}}$ = 6.4 Hz). ^{13}C NMR (CD_2Cl_2, δ ppm): 188.52 (Ru=*C*), 154.81 (Ru-C_{ar}), 153.70 (N-C_{ar}), 145.42 (N-C_{ar}), 141.61 (=C-C_{ar}), 136.95, 131.38, 131.06, 130.93, 130.67, 129.18, 128.80, 128.41, 126.60, 124.53 (Ph, CH_3*C*N), 113.85, 106.34 ($C_{\text{ar}}CH_3$, $C_{ar}CH(CH_3)_2$), 95.47, 93.53, 90.88, 87.84 (*C*H *p*-cym), 31.60 (*C*HMe$_2$), 23.19 (CH($\mathit{C}H_3)_2$), 21.64 (CH($\mathit{C}H_3)_2$), 19.18 (Ar$\mathit{C}H_3$ *p*-cym), 4.30 ($\mathit{C}H_3$CN).

X-ray crystallography

Crystals of **4** suitable for X-ray diffraction analysis were obtained by slow diffusion of *n*-pentane in a CH_2Cl_2 solution at –18°C. A summary of the crystal data and parameters for data collection is given in Table 6. Data were collected at 293 K on a four circle Brucker P4 diffractometer using monochromated Mo K_α radiation (0.71073 Å). The structure was solved by direct method and refinement was performed on F^2 using the SHELXL-96 solution package programs (28). All non-hydrogen atoms were refined anisotropically. Hydrogen atoms were located on difference Fourier map and refined isotropically. Complete tables of bond distances and angles, final atomic coordinates, and anisotropic displacement parameters have been deposited as supplementary material.[2]

Typical polymerization procedure

A ruthenium complex (0.0117 mmol) was placed in a glass tube containing a magnet bar and capped by a three-way stopcock. Air was expelled by three vacuum–nitrogen cycles before methyl methacrylate (1 mL, 9.35 mmol) and the initiator solution (0.1 M in toluene, 0.234 mL) were added. All liquids were handled with dried syringes under nitrogen. The reaction mixture was heated for 16 h at 85°C under inert atmosphere. After cooling, it was diluted with THF and poured in *n*-heptane (600 mL) under vigorous stirring. The precipitated polymer was filtered with suction and dried overnight at 80°C under vacuum.

Styrene and the *p*-substituted styrenes were polymerized according to the same procedure and precipitated from methanol. In all experiments, 1 mL of monomer was used (see the Tables for further information on the initiator, the temperature, and the reaction time).

Table 6. Crystallographic data for complex **4**.

Formula	$C_{30}H_{28}ClN_3Ru$
Formula weight	567.07
Crystal system	Monoclinic
Space group	$P2_1/c$
a (Å)	9.6322(13)
b (Å)	17.970(2)
c (Å)	15.128(2)
α (°)	90
β (°)	107.930(12)
γ (°)	90
V (Å^3)	2491.3(6)
Z	4
$\rho_{\text{calc.}}$ (g cm^{-3})	1.512
μ (mm^{-1})	0.761
F(000)	1160
Crystal size (mm)	0.30 × 0.4 × 0.35
Temperature (K)	293(2)
2θ limits (°)	1.8–25.0
Total reflections	5543
Unique reflections	4350
No. of variables	428
Goodness-of-fit	1.019
R_1 [$I > 2\sigma(I)$]^a	0.0285
wR_2 (all data)^b	0.0692
Max, min resid. density (e Å^{-3})	1.362 and –0.495

$^aR_1 = \Sigma||F_0| - |F_c||\Sigma|F_0|$.
$^bwR_2 = [\Sigma[w(F_0^2 - F_c^2)^2]/\Sigma[w(F_0^2)_2]]^{0.5}$.

Polymer characterization

Molecular weight distributions were determined by SEC in THF at 40°C using a Hewlett–Packard 1090 liquid chromatograph equipped with a Hewlett–Packard 1037A refractive index detector. PMMA and PS standards (Polymer Laboratories) were used for calibration. Before SEC analysis, the polymers were purified by passing solutions through a short Al_2O_3-filled column. ^{1}H NMR spectra were recorded at room temperature in $CDCl_3$ with TMS as internal reference on a Brucker AM 400 apparatus.

Conclusions

A major advantage of utilizing transition-metal complexes as catalysts is the possibility to fine tune their electronic and steric properties through the design of their ligands. Our research on the potential of various ruthenium(II)-phosphine or ruthenium(II)-triazolinylidene complexes to promote atom transfer radical polymerization of vinyl monomers nicely illustrates this concept. Polymerizations of methyl methacrylate and of styrene were chosen as model reactions with ethyl 2-bromo-(2-methyl)propanoate or (1-chloroethyl)benzene serving as initiators. Very efficient catalyst precursors were

---

[2] Copies of material on deposit may be purchased from the Depository of Unpublished Data, Document Delivery, CISTI, National Research Council Canada, Ottawa, Ontario, Canada K1A OS2 ((http://www.nrc.ca/cisti/irm/unpub_e.shtml for information on ordering electronically). Copies of the data can be obtained, free of charge, on application to the Director, CCDC, 12 Union Road, Cambridge CB2 1EZ, U.K. (Fax: 44-1223-336033 or e-mail: deposit@ccdc.cam.ac.uk).

obtained when bulky and basic phosphines were ligated to the metal. Ligands that did not meet these requirements gave much poorer or inefficient catalyst systems for ATRP.

Acknowledgments

Financial support from the Fonds National de la Recherche Scientifique (F.N.R.S.), Belgium, for the purchase of major instrumentation is gratefully acknowledged. We also thank the EU TMR program (HPRN-CT-2000-10) for generous support.

References

1. M. Sawamoto and M. Kamigaito. CHEMTECH. June, 30 (1999).
2. K. Matyjaszewski. *In* Education in advanced chemistry, mechanistic aspects of molecular catalysis. Vol. 6. *Edited by* K. Matyjaszewski. and B. Marciniec. Wydawnictwo Poznanskie, Poznan-Wroclaw. 1999. pp. 95–105.
3. K. Matyjaszewski (*Editor*). Controlled/living radical polymerization: Progress in ATRP, NMP, and RAFT. Vol. 768. ACS Symposium Series. ACS, Washington, D.C. 2000.
4. K. Matyjaszewski. Chem. Eur. J. **5**, 3095 (1999).
5. C.J. Hawker. Acc. Chem. Res. **30**, 373 (1997).
6. M. Sawamoto and M. Kamigaito. *In* Materials science and technology. A comprehensive treatment. *Edited by* R.W. Cahn, P. Haasen, and E.J. Kramer. Synthesis of polymers. A.-D. Schlüter (*Volume Editor*). Wiley-VCH, Weinheim. 1999. pp. 163–194.
7. K. Matyjaszewski. Macromolecules **31**, 4710 (1998); Macromolecules **31**, 4718 (1998).
8. D.M. Haddleton, M.C. Crossman, B.H. Dana, D.J. Duncalf, A.M. Heming, D. Kukulj, and A.J. Shooter. Macromolecules **32**, 2110 (1999).
9. H. Uegaki, Y. Kotani, M. Kamigaito, and M. Sawamoto. Macromolecules **30**, 2249 (1997).
10. T. Ando, M. Kamigaito, and M. Sawamoto. Macromolecules **30**, 4507 (1997).
11. F. Simal, A. Demonceau, and A.F. Noels. Angew. Chem. Int. Ed. Engl. **38**, 538 (1999).
12. A. Demonceau, A.W. Stumpf, E. Saive, and A.F. Noels. Macromolecules **30**, 3127 (1997).
13. D. Jan, L. Delaude, F. Simal, A. Demonceau, and A.F. Noels. J. Organomet. Chem. **606**, 55 (2000).
14. K.J. Ivin and J.C. Mol. Olefin metathesis and metathesis polymerization. Academic Press Ltd., London. 1997.
15. A. Amir-Ebrahimi, D.A. Corry, J.G. Hamilton, J.M. Thompson, and J.J. Rooney. Macromolecules **33**, 717 (2000).
16. F. Simal, A. Demonceau, and A.F. Noels. Tetrahedron Lett. **40**, 5689 (1999).
17. F. Simal, A. Demonceau, A.F. Noels, F. Kohl, T. Weskamp, and W.A. Herrmann. Chem. Eur. J. **7** (2001) accepted for publication.
18. D. White and N.J. Coville. Adv. Organomet. Chem. **36**, 95 (1994).
19. W.A. Henderson, Jr. and C.A. Streuli. J. Am. Chem. Soc. **82**, 5791 (1960).
20. G. Moineau, P. Dubois, R. Jérôme, T. Senninger, and P. Teyssié. Macromolecules **31**, 545 (1998).
21. F. Simal, L. Delaude, D. Jan, A. Demonceau, and A.F. Noels. Polym. Prepr. (Am. Chem. Soc. Div. Polym. Chem.) **40**, 336 (1999).
22. J. March. Advanced organic chemistry. 3rd ed. Wiley-Interscience, New York. 1985. pp. 242–250.
23. T. Weskamp, V.P.W. Böhm, and W. A. Herrmann. J. Organomet. Chem. **600**, 12 (2000).
24. D. Enders, K. Breuer, G. Raabe, J. Runsink, J.H. Teles, J.P. Melder, K. Ebel, and S. Brode. Angew. Chem. Int. Ed. Engl. **34**, 1021 (1995).
25. H. Enders, H. Gielen, G. Raabe, J. Runsink, and J.H. Teles. Chem. Ber./Recl. **130**, 1253 (1997) and refs. cited therein.
26. J. Huang, E.D. Stevens, S.P. Nolan, and J.L. Petersen. J. Am. Chem. Soc. **121**, 2674 (1999).
27. T. Weskamp, W.C. Schattenmann, M. Spiegler, and W.A. Herrmann. Angew. Chem. Int. Ed. Engl. **37**, 2490 (1998).
28. G. Sheldrick. SHELXL-96. University of Göttingen, Göttingen, Germany. 1996.